nature
structural biology

Germline antibody recognition of distinct carbohydrate epitopes

Hoa P Nguyen[1], Nina O L Seto[1,2], C Roger MacKenzie[2], Lore Brade[3], Paul Kosma[4], Helmut Brade[3] & Stephen V Evans[1,5]

High-resolution structures reveal how a germline antibody can recognize a range of clinically relevant carbohydrate epitopes. The germline response to a carbohydrate immunogen can be critical to survivability, with selection for antibody gene segments that both confer protection against common pathogens and retain the flexibility to adapt to new disease organisms. We show here that antibody S25-2 binds several distinct inner-core epitopes of bacterial lipopolysaccharides (LPSs) by linking an inherited monosaccharide residue binding site with a subset of complementarity-determining regions (CDRs) of limited flexibility positioned to recognize the remainder of an array of different epitopes. This strategy allows germline antibodies to adapt to different epitopes while minimizing entropic penalties associated with the immobilization of labile CDRs upon binding of antigen, and provides insight into the link between the genetic origin of individual CDRs and their respective roles in antigen recognition.

The initial immune response to a new carbohydrate epitope arises largely from antibodies constructed from germline gene segments; however, the molecular basis underlying the mechanism by which a germline antibody recognizes a range of epitopes has been a subject of debate for decades. Germline gene segments have evolved to confer immunity to common pathogens, and the introduction of a new pathogen has the potential to decimate a population. Additionally, the ability of germline antibodies to adapt to new pathogens has been a central aspect of antibody theory, from the template instruction theory[1,2] to the clonal selection theory[3–7]. To promote the survival of the organism, the portion of the germline dedicated to humoral response must balance between antibody segments that show the greatest adaptability to new pathogens with those segments that convey hereditary immunity to common pathogens.

The repertoire of germline gene segments is a critical consideration for carbohydrate-specific antibodies (which generally do not undergo class switching and affinity maturation) in immune surveillance for microbial pathogenesis and diseased tissue. The observed low affinity of antibodies to oligosaccharides has limited the study of the three-dimensional mechanisms of specificity of antibodies to carbohydrates, and there exist just a few reports of the structures of antibody fragments in complex with carbohydrate antigen[8–12]. Progress has been further limited because these reports consist largely of unrelated antibodies that are specific for markedly different oligosaccharide epitopes. This paucity in structural data has prevented an assessment of the relative contributions of germline gene segments to the recognition of bacterial carbohydrate epitopes. Here we have selected from an extensive library of monoclonal antibodies (mAbs) two highly homologous antibodies constructed largely from germline gene segments that recognize several distinct highly conserved epitopes of bacterial LPS.

Bacterial LPS is a major antigenic surface feature for all Gram-negative bacteria and generally consists of a lipid A moiety to which an inner core oligosaccharide consisting of 3-deoxy-D-manno-oct-2-ulosonic acid (Kdo), an outer core region of heptoses and hexoses, and the polysaccharide O-antigen are successively attached. Chlamydial LPS and rough Re-type LPS found in enterobacterial genera including *Salmonella*, *Escherichia* and *Proteus* are truncated, lacking both the outer core and the O-antigen[13–15]. The inner core oligosaccharide of Re-type LPS features a Kdo disaccharide epitope αKdo(2→4)-αKdo (**Fig. 1a**), the smallest LPS structure required to maintain bacterial membrane barrier functions[13,14]. A unique Kdo trisaccharide epitope, αKdo(2→8)-αKdo(2→4)-αKdo (**Fig. 1a**), is present in all species of the Chlamydiaceae family but has not been observed in any other bacterium, and is thus an important taxonomic and diagnostic marker. One species, *Chlamydophila psittaci*, also shows the trisaccharide epitope αKdo(2→4)-αKdo(2→4)-αKdo in addition to the family-specific epitope[16]. Members of the bacterial family Chlamydiaceae are obligatory intracellular pathogens. *Chlamydia trachomatis* is a leading cause of preventable blindness[17], sexually transmitted infection of the urogenital tract and acquired infertility[18], and is also known to cause

[1]Department of Biochemistry, Microbiology and Immunology, University of Ottawa, 451 Smyth Road, Ottawa, Ontario K1H 8M5, Canada. [2]National Research Council of Canada, Institute for Biological Sciences, 100 Sussex Drive, Ottawa, Ontario K1A 0R6, Canada. [3]Division of Medical and Biochemical Microbiology, Research Center Borstel, Center for Medicine and Biosciences, Parkallee 1-40, D-23845 Borstel, Germany. [4]Institute of Chemistry, University of Agriculture, A-1190 Vienna, Austria. [5]Department of Biochemistry and Microbiology, University of Victoria, PO Box 3800, STN CSC, Victoria, British Columbia V8W 3P6, Canada. Correspondence should be addressed to S.V.E. (svevans@uvic.ca).

Published online 16 November 2003; doi:10.1038/nsb1014

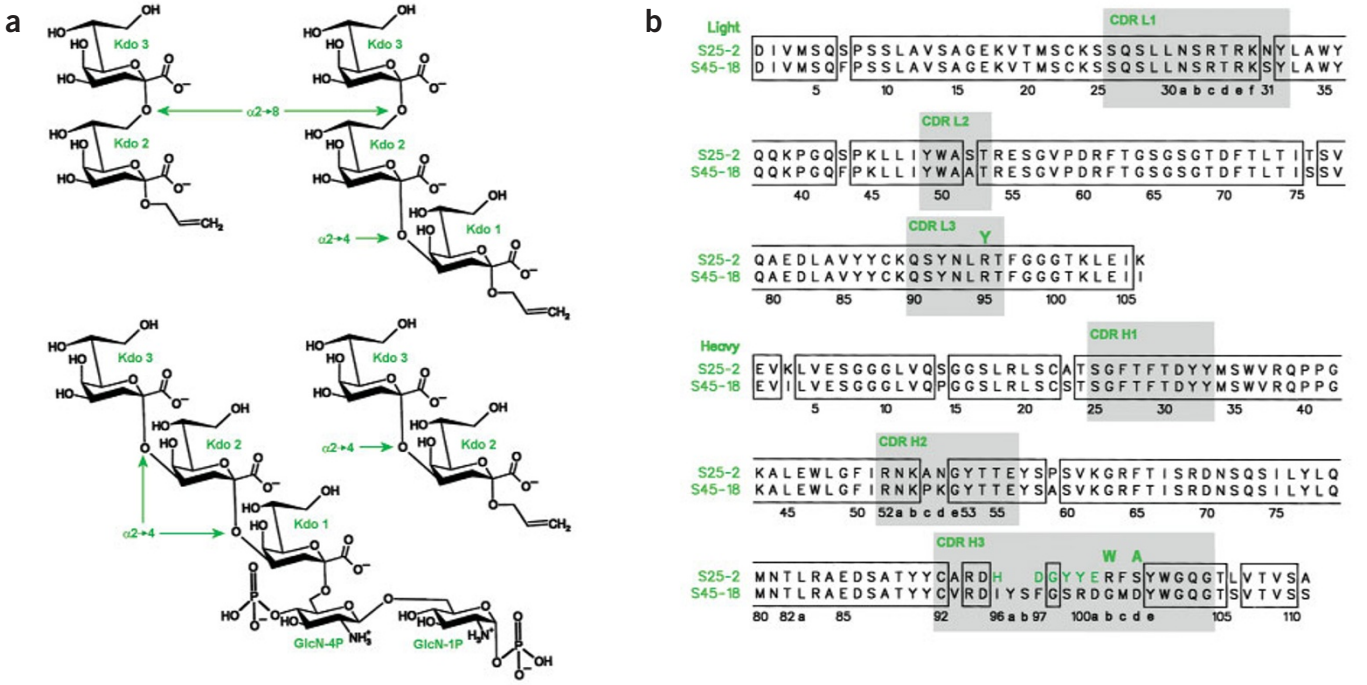

Figure 1 Chemical structures of antigens and antibodies. (**a**) α(2→8) antigens αKdo(2→8)–αKdo(2→O-allyl) disaccharide (top left), αKdo(2→8)-αKdo(2→4)-αKdo(2→O-allyl) trisaccharide antigens (top right) and αKdo(2→4)-αKdo(2→O-allyl) disaccharide (bottom right) were crystallized with S25-2; and pentasaccharide antigen αKdo(2→4)-αKdo(2→4)-αKdo(2→6)-βGlcN-4P(1→6)-αGlcN-1P (bottom left) was crystallized with S45-18. Figure produced using ChemSketch (Advanced Chemistry Developments). (**b**) Amino acid sequence alignment of S25-2 and S45-18 variable domains with the CDRs shaded. The numbering is based on studies by Chothia[42,43,46] and the online Kabat database (http://www.rubic.rdg.ac.uk/abs/simkab.html)[58]. The residues in bold above the sequence alignment shows where S25-2 differs from germline in the regions encoded by the V and J immunoglobulin genes. The sequences encoded by the D minigenes are highlighted in green.

pneumonitis and urogenital tract infections in mice[19]. *Chlamydophila pneumoniae* causes infections of the respiratory tract[20] and has been linked to bronchial asthma[21], heart disease[22–24], multiple sclerosis and Alzheimer's disease[25]. The ubiquitous nature of these LPS epitopes has made them high-profile targets for vaccine development[26–28].

S25-2 is a mAb with affinity for the chlamydial family-specific terminal α(2→8)-linked Kdo residues and binds the trisaccharide αKdo(2→8)-αKdo(2→4)-αKdo against which it was raised[29]. Notably, S25-2 also binds the partial chlamydial epitope αKdo(2→8)-αKdo and the Re-type epitope αKdo(2→4)-αKdo disaccharides[30]. The mAb S45-18 is specific for the trisaccharide αKdo(2→4)-αKdo(2→4)-αKdo and does not bind to the αKdo(2→8)-αKdo(2→4)-αKdo trisaccharide epitope[16].

A comparison of the polypeptide sequences of S25-2 with known murine germline sequences shows that S25-2 corresponds to the germline genes IGKV8-21 Y15982, IGKJ2 V00777, IGHV7S3 J00525 and IGHJ3 V00770 (IMGT, the international ImMunoGeneTics database, http://imgt.cines.fr; initiator and coordinator, Marie-Paule Lefranc, Montpellier, France) with only three mutations: Y95R (light chain), W100bR (heavy chain, **Fig. 1b**) and A100dS (heavy chain, **Fig. 1b**). S45-18 has additional mutations away from germline, including six residues in the light chain and seven in the heavy chain, not including the D region. CDRs L3 and H1 are common between S25-2 and S45-18, whereas CDRs L1, L2 and H2 have one or two changes in residue identity with no change of CDR length. The most important differences between S45-18 and S25-2 lie in CDRs H3 (ref. 31), which are based on different germline gene segments such as IGHJ4 V00770 in S45-18 (**Fig. 1a**), and the 'D' region, which is prone to mutation. Specifically, the sequence of S45-18 has more mutations away from germline, and the 'JH' region is encoded by a different germline gene. Unlike other CDRs, H3 is formed by two joining events involving the D (diversity) minigenes. During each rearrangement the flanking regions of the genes involved can undergo addition and deletion of nucleotides, and duplication of the D gene can also occur[32]. Mutation of germline sequences and the structural basis for improvement of affinity for protein antigen have been studied recently[33]; however, no corresponding model for carbohydrate recognition has been reported.

We have determined the structures of Fabs from both antibodies to high resolution in the presence and absence of several epitopes in order to establish the three-dimensional nature of a hereditary murine germline response to a carbohydrate epitope of a bacterial pathogen, the manner by which such a site can accommodate several distinct epitopes and the pathway by which the substitution of a few residues can transform the low-specificity S25-2 into the highly specific S45-18.

RESULTS

The Fab from mAb S25-2 has been crystallized in complex with 2→O-allyl derivatives containing the α(2→8)-α(2→4) Kdo trisaccharide, α(2→8) Kdo disaccharide, α(2→4) Kdo disaccharide epitopes and the Kdo monosaccharide, and unliganded in two different crystal forms. The Fab from mAb S45-18 has been crystallized in complex with the deacylated LPS pentasaccharide antigen αKdo(2→4)-αKdo(2→4)-αKdo(2→6)-βGlcN-4P(1→6)-αGlcN-1P containing the α(2→4)-α(2→4) Kdo trisaccharide epitope as well as in the unliganded form. Data have been collected from 1.49 to 2.2 Å resolution (**Table 1**). All of the CDRs and most of the polypeptide chains show excellent electron density, although CDR H3 of S25-2 shows high thermal motion in the unliganded structures and in the

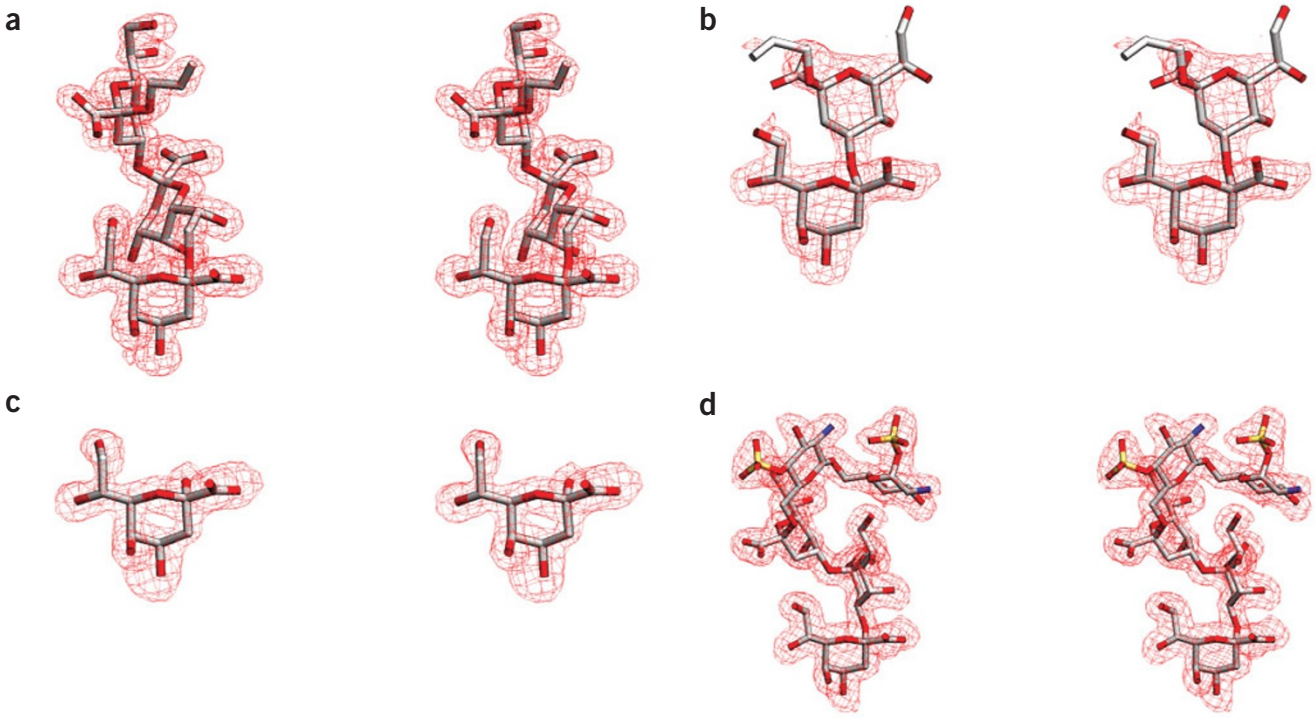

Figure 2 Observed $2F_o - F_c$ σ_A-weighted electron density maps for selected liganded antigens, contoured at 1.0 σ. (**a**) α(2→8)-α(2→4) Kdo trisaccharide bound by S25-2. (**b**) α(2→4) Kdo disaccharide bound by S25-2. (**c**) The Kdo monosaccharide bound by S25-2. (**d**) The pentasaccharide bound by S45-18. **Figures 2–4** were produced using SETOR[57].

α(2→4) disaccharide and monosaccharide complexes. Well-defined electron density is observed for all antigen Kdo residues (**Fig. 2a–d**). The pentasaccharide antigen cocrystallized with S45-18 (**Fig. 1a**) contains two glucosamine phosphate residues that lie in excellent electron density in one of the two Fab molecules in the asymmetric unit of the liganded structure. These residues do not form part of the epitope and are not observed to contact the parent Fab, although they form a hydrogen bond to a water molecule that bridges to an adjacent Fab. The Kdo residues of the monosaccharide complex and α(2→8) disaccharide complex with S25-2 lie in the same position and conformation as the corresponding Kdo residues of the α(2→8)-α(2→4) trisaccharide complex. In general, antibody recognition of carbohydrate antigens has been observed to include a large number of stacking interactions[9,11]; however, antigen recognition in each S25-2 complex is dominated by hydrogen bonds, with only one residue (PheH97 (H, heavy chain)) forming substantial stacking interactions in the S45-18 complex.

Inherited terminal Kdo recognition site

All liganded S25-2 and S45-18 structures show a similar terminal Kdo (Kdo3) binding site made from CDRs L3, H1, H2 and H3 (**Fig. 3a**). The residues contacting Kdo3 in mAb S25-2 correspond to those found in known germline segments with the exception of ArgL95 (L, light chain), which is tyrosine in the germline; however, residue L95 occurs at the junction of two germline segments and is thus prone to mutation[32]. To allow the antibodies to bind several distinct epitopes, the Kdo3 binding site itself shows some flexibility in antigen positioning, because there is among the various complexes a 0.7-Å shift of Kdo3 which is accomplished while maintaining largely the same set of hydrogen bonds. The homologous antibody S45-18 recognizes Kdo3 of the α(2→4)-α(2→4) Kdo epitope using many of the corresponding residues (**Fig 3a**, bottom); however, S45-18 prevents this shift (and so decreases the ability to recognize the α(2→8) disaccharide) by the mutation of GluH100a to aspartate (**Fig. 1b**) and the insertion of a buried bridging water molecule (**Fig. 3a**). This bridging water molecule is also present in the unliganded S45-18 structure, though exposed to the solvent.

The flexibility of the common Kdo3 binding site in the S25-2 and S45-18 complexes is further illustrated by the conservation of two water molecules that bridge identical contacts between antibody and antigen yet are observed to shift position by 1.8 Å between the complexes.

S25-2 uses the same residues to recognize different epitopes

Although all complexes show Kdo3 as occupying similar positions in the binding site, the corresponding Kdo2 residues lie in markedly different conformations, and several corresponding amino acid residues show multiple functionalities (**Fig. 3b**). Specifically, TyrH33 forms a hydrogen bond to O5 of Kdo2 in the α(2→4) disaccharide but forms a hydrogen bond to O7 in the α(2→8)-α(2→4) trisaccharide complex. AsnH52d forms a hydrogen bond with O7 of Kdo2 in both complexes, even though Kdo2 lies in considerably different conformations in each complex. ArgL30c forms a bidentate salt bridge with the carboxylate of Kdo2 in the α(2→4) disaccharide complex but forms a hydrogen bond to Kdo1 O5 in the α(2→8)-α(2→4) trisaccharide (**Fig. 3b**). Finally, although water molecules are observed bridging the protein and Kdo2 in the α(2→8) complex, no ordered water molecules are observed about the α(2→4) disaccharide.

Swapping CDR H3 markedly changes specificity

Antibody S45-18 was raised against the α(2→4)-α(2→4) Kdo trisaccharide and is virtually homologous to S25-2 with the exception of

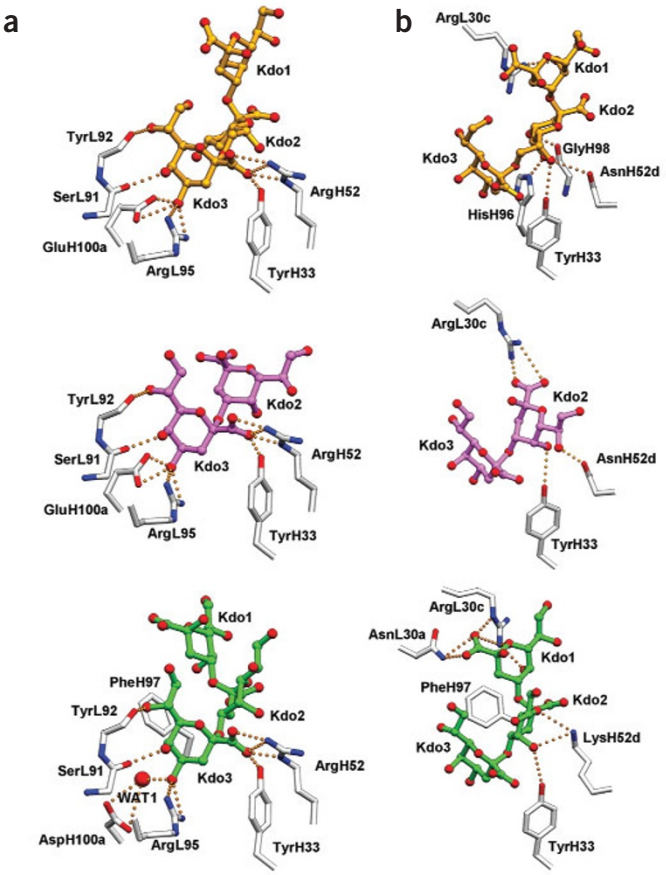

Figure 3 Binding environments for representative liganded antigens. The α(2→8)-α(2→4) trisaccharide bound to S25-2 is yellow, the α(2→4) disaccharide bound to S25-2 is magenta and the α(2→4)-α(2→4) trisaccharide of the pentasaccharide antigen bound to S45-18 is green. (**a**) All complexes share a related terminal Kdo binding pocket. (**b**) S25-2 shows flexibility in binding the remaining Kdo residues in range of distinct epitopes, whereas S45-18 uses a different CDR H3 to specifically recognize one antigen.

CDR H3, which arises from a different germline gene (**Fig. 1b**). However, unlike S25-2, S45-18 shows high specificity and is not observed to bind to any other epitope. The ability of a related set of antigens to elicit an antibody response from a restricted set of germline genes is common[34–38] and demonstrates the potential to combine the inherited terminal Kdo binding site with different CDR H3 loops to change and constrain the specificity toward a particular epitope.

The higher specificity of S45-18 stems from several factors. In addition to the change in Kdo3 binding caused by the E100aD (heavy chain, **Fig. 1b**) mutation, the longer length and altered sequence results in the projection of the bulk of PheH97 into the binding site (**Fig. 3a**,**b**), where it forms van der Waals contacts (so-called stacking interactions) with all three hexose rings of the α(2→4)-α(2→4) trisaccharide. The presence of PheH97 also precludes the binding of an α(2→8)-linked Kdo2 residue and forces the rearrangement of the conformation of Kdo2 from that observed in the S25-2 α(2→4) disaccharide complex. The mutation N52dK (heavy chain, **Fig. 1**) in S45-18 allows hydrogen bonds to form between the lysine and O6 and O7 of Kdo2, respectively. AsnL30a and ArgL30c show the same diverse functionality observed in complexes of S25-2 by forming several hydrogen bonds to Kdo1 (**Fig. 3b**). In fact, ArgL30c forms hydrogen bonds with a different antigen moiety in each of the complex structures in which it participates.

These are the first reported examples of an antigen-binding fragment crystallized with a carbohydrate antigen having charged groups, and notably, almost all the antigen's carboxylic acid moieties form salt bridges in the liganded structures. The charged glucosamine phosphate residues linked to the α(2→4)-α(2→4) trisaccharide in S45-18 are not observed to form interactions with any protein atoms.

DISCUSSION

The most marked aspect of these complexes is the facility of mAb S25-2 to recognize the distinct carbohydrate epitopes formed by different glycosidic linkages. S25-2 and S45-18 both use one portion of the combining site to recognize the terminal Kdo (Kdo3) in each epitope in the same way and with high specificity, whereas the rest of the combining site adapts to or excludes the remainder of the different epitopes. Because the sequence of S25-2, and to a lesser extent that of S45-18, corresponds to germline segments, these structures offer insight into the balance found in inherited germline gene segments between the maintenance of immunity to common pathogens and the flexibility to recognize new pathogens.

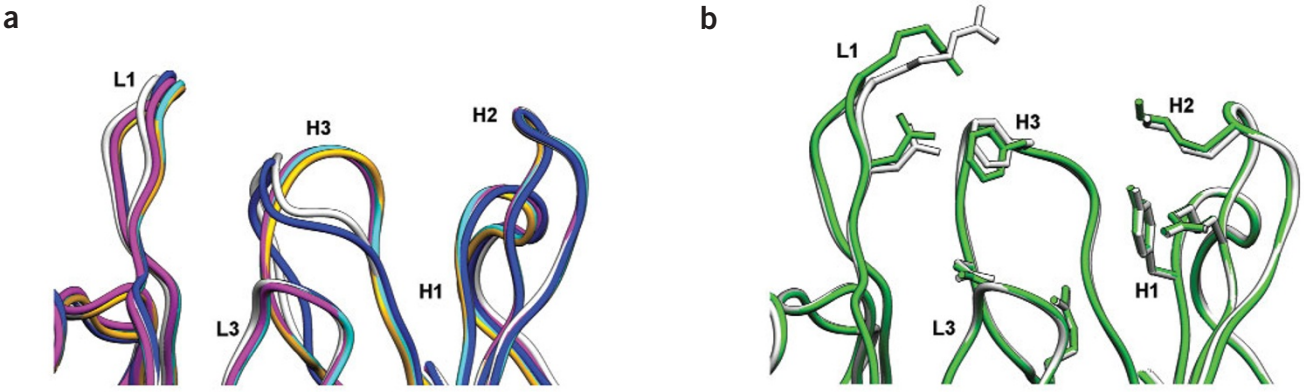

Figure 4 Conformational variation observed among liganded and unliganded forms of S25-2 and S45-18. (**a**) Overlap of unliganded S25-2 (crystal form 1, dark blue; crystal form 2, white), S25-2 bound to α(2→8)-α(2→4) trisaccharide (yellow), S25-2 bound to α(2→4) disaccharide (magenta) and S25-2 bound to the Kdo monosaccharide (cyan). The trace of the α(2→8) disaccharide complex is similar to the α(2→8)-α(2→4) trisaccharide complex and is not shown. (**b**) Overlap of unliganded (white) and liganded (green) S45-18.

Table 1 Data refinement and model statistics for unliganded and liganded forms of S25-2 Fab and S48-18 Fab

	S25-2 Fab						S45-18 Fab	
	Unliganded form 1	Unliganded form 2	α(2→8)-α(2→4) trisaccharide	α(2→8) disaccharide	α(2→4) disaccharide	Monosaccharide	Unliganded	Pentasaccharide
Data collection								
Space group	$P2_12_12$	$P2_12_12_1$	$P2_12_12_1$	$P2_12_12_1$	$P2_12_12_1$	$P2_12_12_1$	$C2$	$P2_12_12_1$
Unit cell dimensions								
a (Å)	96.8	84.7	45.6	45.9	45.9	45.9	76.4	71.2
b (Å)	112.2	96.0	80.9	81.6	81.8	81.8	170.3	113.9
c (Å)	41.5	114.2	130.6	131.5	130.3	130.3	77.1	133.9
β (°)	114.4							
Molecules per asymmetric unit	1	2	1	1	1	1	2	2
Refinement								
Observations	203,789	230,670	279,457	870,735	363,226	183,080	234,850	406,104
Unique reflections[a]	31,851 (2,827)	38,076 (3,282)	77,711 (6,994)	84,235 (8,455)	49,410 (4,918)	44,748 (4,791)	75,932 (6,553)	106,111 (10,237)
Resolution range (Å)	20–1.96	20–2.28	20–1.49	20–1.45	20–1.74	20–1.73	20–1.79	20–1.75
Completeness (%)[a]	96.1 (87.5)	88.4 (77.5)	97.3 (88.9)	95.2 (96.9)	97.9 (96.4)	92.3 (84.8)	90.4 (78.5)	95.8 (93.1)
R_{sym}[a,b]	0.054 (0.328)	0.053 (0.380)	0.042 (0.398)	0.051 (0.247)	0.043 (0.381)	0.043 (0.353)	0.030 (0.133)	0.063 (0.396)
$\langle I / \sigma (I) \rangle$[a]	28.3 (3.2)	29.7 (4.2)	29.9 (2.3)	38.1 (9.4)	40.5 (3.9)	22.7 (3.2)	41.6 (6.9)	18.2 (2.4)
Number of atoms								
Polypeptide[c]	3,399	6,798	3,399	3,399	3,413	3,399	6,850	6,850
Sugar[c]	0	0	49	34	34	16	0	136
Solvent[c]	273	409	473	516	339	397	529	770
R_{work}[d]	0.223	0.216	0.200	0.203	0.215	0.202	0.220	0.212
R_{free}[d]	0.275	0.287	0.223	0.225	0.252	0.236	0.247	0.247

[a]Values in parentheses refer to the highest-resolution shell, which corresponds to 2.03–1.96 Å for S25-2 unliganded form 1, 2.36–2.28 Å for S25-2 unliganded form 2, 1.54–1.49 Å for the S25-2 α(2→8)-α(2→4) trisaccharide, 1.50–1.45 Å for the S25-2 α(2→8) disaccharide, 1.80–1.74 Å for the S25-2 α(2→4) disaccharide, 1.79–1.73 Å for the S25-2 monosaccharide, 1.85–1.79 Å for unliganded S45-18 and 1.81–1.75 Å for liganded S45-18. [b]$R_{sym} = \Sigma|(I_{hkl} - I_{<hkl>})| / (\Sigma I_{hkl})$ where $I_{<hkl>}$ is the mean intensity of all reflections equivalent to reflection *hkl* by symmetry. [c]Nonhydrogen atoms. [d]R_{work}, $R_{free} = \Sigma ||F_o| - |F_c|| / \Sigma |F_o|$; 10% of the data was used for the calculation of R_{free}.

Heredity versus adaptability

In addition to the use of many amino acid residues in binding to ligand, mAb S25-2 shows substantial flexibility in the conformation of CDR H3 (and to a lesser extent L1), between the liganded and unliganded forms (**Fig. 4a**). The four liganded forms have approximately the same conformation, which is different from that of the two unliganded forms, and shows that S25-2 undergoes a significant induced fit upon antigen binding. In contrast, the more specific S45-18 shows little induced fit (**Fig. 4b**).

The observation of an antibody corresponding to germline sequence showing substantial flexibility has fundamental implications when considering the competing aspects in antigen recognition by germline antibodies. The inherited germline antibody response can be critical, and animals typically carry hereditary resistance to common pathogens. This is important for carbohydrate antigens, which usually cannot induce T-cell help and stimulate the production of antibodies with higher affinities. In addition, germline antibodies in general must also exhibit some flexibility to cope with new or changing pathogen surface structures. However, any advantage of flexibility can be offset by the large entropic penalty incurred by the immobilization of labile antibody CDR loops.

S25-2 shows how a germline antibody could achieve this balance by coding for the recognition of the terminal Kdo residue using CDRs with stable conformations while leaving the rest of the combining site to either exhibit flexibility or impose specificity. Such a strategy allows this antibody to recognize several epitopes showing the terminal Kdo residue without the entropic penalties of a more flexible combining site. Antibody S45-18 shows how removing this adaptability can lead to an antibody of higher specificity.

The original concept of the highly adaptable germline antibody of the template instruction theory[1,2] was abandoned when clonal selection was found to be the basis of antibody response[3–7]; however, it is becoming increasingly apparent that flexibility is a key aspect of germline antibody recognition[39–41] when coupled to hereditary recognition of pathogen epitopes.

Canonical forms, inherited binding sites and CDR H3

H3 has a unique genetic origin among the murine CDRs. Whereas L1, L2, L3, H1 and H2 correspond closely to a few germline sequences, H3 displays a substantially higher level of sequence variation due to the insertion of D minigenes (reviewed in ref. 32; **Fig. 1b**). These D genes comprise 11–23 base pairs and during genetic rearrangement can undergo duplication with the flanking regions of the genes subject to high levels of mutation. This nonencoded sequence variation contributes to the special properties observed for H3.

For example, one of the seminal advances in the prediction of protein structure was the characterization of the canonical conformations of most of the CDRs by Chothia and Lesk[42–47]; however, a successful methodology for the prediction of the conformation of CDR H3 remained elusive for many years. This became increasingly frustrating as reports mounted of the importance of H3 in determining antigen specificity[40,48–50]. Important headway in predicting H3 conformation was reported by Nakamura in 1996 (ref. 49); however, S25-2 exemplifies the reason that H3 remains difficult. Using Nakamura's method,

CDR H3 of S45-18 corresponds to one of the new canonical forms, as does H3 of the structure of the liganded S25-2 (ref. 49); however, the conformation of H3 in the unliganded form of S25-2 is still not predicted from its sequence. Notably, the single hydrogen bond formed between GluH100a and Kdo O4 in the structure of S25-2 bound to Kdo monosaccharide is sufficient to convert CDR H3 from an unpredicted form to a predicted form.

Finally, the structures of S25-2 and S45-18 offer insight into an evolutionary strategy behind the observed high sequence variation in H3, illustrating the requirement that antibody germline sequences possess a balance between inherited immunity and the ability to respond to new pathogens. Both of these antibodies reveal in this case that inherited immunity is provided largely by CDR loops that are known to have greater genetic and conformational stability, whereas the determination of specificity (or lack thereof) is made by the more variable and flexible H3. It seems probable that this is a general strategy for other classes of epitopes, because the combination of the inherited terminal Kdo binding site in these mAbs provided by L3, H1 and H2 and with different H3 loops gives the ability to produce efficiently both antibodies that are specific for a range of related Kdo epitopes as well as antibodies that have high specificity.

METHODS

Purification and crystallization of Fab. The production of IgG S25-2 and IgG S45-18 has been described[16,29], as has the isolation and purification of the corresponding Fabs[31]. S25-2 Fab was crystallized without ligand, in complex with a synthetic trisaccharide analog of the family-specific epitope αKdo(2→8)-αKdo(2→4)-αKdo(2→O-allyl), and also with two synthetic disaccharides, αKdo(2→8)-αKdo(2→O-allyl) and αKdo(2→4)-αKdo (2→O-allyl) and Kdo monosaccharide (Kdo ammonium salt, K2755 from Sigma) corresponding to its partial epitopes. The chemical identities of the carbohydrate LPS components were deduced from earlier studies[51,52], and the synthetic analogs were shown to mimic their natural counterparts[29]. S45-18 Fab has been crystallized without ligand and in complex with the deacylated LPS pentasaccharide bisphosphate antigen αKdo(2→4) -αKdo(2→4)-αKdo(2→6)-βGlcN-4P(1→6)-αGlcN-1P. The crystals were grown by the hanging-drop vapor diffusion method in the presence of 80-fold molar excess of antigen to Fab under the conditions reported[31], with the exception of S25-2 Fab in complex with the αKdo(2→4)-αKdo(2→O-allyl) disaccharide (18 mg ml^{-1} Fab, ~100-fold molar excess antigen, 40 mM $MgCl_2$, 30 mM $ZnCl_2$, 8% (w/v) PEG 4000, 11% (w/v) ethylene glycol, 20 mM Tris, pH ~8, over a reservoir containing 200 mM $MgCl_2$, 25% (w/v) PEG 4000, 100 mM Tris, pH 8.5) and Kdo monosaccharide (15 mg ml^{-1} Fab, ~150-fold molar excess antigen, 40 mM $MgCl_2$, 20 mM $ZnCl_2$, 7% (w/v) PEG 4000, 9% (w/v) ethylene glycol, 20 mM Tris, pH ~8, over a reservoir of 200 mM $MgCl_2$, 25% (w/v) PEG 4000, 100 mM Tris, pH 8.5).

Data collection. Data was collected at wavelength 1.15 Å at Brookhaven National Laboratories (Upton, New York, USA) at the National Synchrotron Light Source (NSLS) beamline X8C (Area Detector Systems Corporation Quantum 4Q CCD detector; Oxford Cryosystems Model 600 low-temperature system). DENZO and SCALEPACK were used as part of the HKL 2000 package[53] for data integration and scaling.

Structure determination. Molecular replacement (MR) and refinement were conducted using CNS[54] with the variable domain of the unliganded YsT9.1 Fab (PDB entry 1MAM)[55,56] initially as the search model for the unliganded S45-18 Fab. Rigid-body, simulated annealing, positional and *B*-factor refinements were carried out using CNS. SETOR[57] and PyMol (DeLano Scientific; http://www.pymol.org) were used for manual fitting of σ_A-weighted $2F_o - F_c$ and $F_o - F_c$ electron density maps. The refined structure of unliganded S45-18 Fab was then used as a search model for the remaining S45-18 and S25-2 liganded structures. Unambiguous MR solutions were found for each data set using the CNS scripts provided for rotation, translation and translation-dimer searches. The diffraction data and model statistics are given in **Table 1**.

Coordinates. Atomic coordinates have been deposited in the Protein Data Bank S25-2 unliganded forms 1 and 2 (accession codes 1Q9K and 1Q9L, respectively); S25-2 in complex with α(2→8)-α(2→4) Kdo trisaccharide, α(2→8) Kdo disaccharide, α(2→4) Kdo disaccharide and Kdo monosaccharide (accession codes 1Q9Q, 1Q9R, 1Q9T and 1Q9V, respectively); and S45-18 unliganded and in complex with the pentasaccharide containing the α(2→4)-α(2→4) Kdo trisaccharide (accession codes 1Q9O and 1Q9W, respectively).

ACKNOWLEDGMENTS

S.V.E. thanks the Natural Sciences and Engineering Research Council of Canada for operating funding and funding for beamline access, and the Canadian Institutes of Health Research for salary support. H.B. and L.B. thank the Deutsche Forschungsgemeinschaft for financial support. P.K. thanks Fonds zur Förderung der wissenschaftlichen Forschung for financial assistance. We thank D.R. Bundle at the University of Alberta and E.Brown at the University of Ottawa for helpful discussions, T.-D. Nguyen, V. Susott, U. Agge and S. Cohrs for technical assistance and the National Synchrotron Light Source staff at beamlines X8C and X12C at Brookhaven National Laboratories, which is supported by the US Department of Energy, Division of Materials Sciences and Division of Chemical Sciences.

COMPETING INTERESTS STATEMENT

The authors declare that they have no competing financial interests.

Received 25 June; accepted 9 October 2003
Published online at http://www.nature.com/naturestructuralbiology/

1. Breinl, F. & Haurowitz, F. Chemische Untersüchung des Präzipitates aus Haemoglobin und Anti-Haemoglobin-Serum und Bemerkungen über die Nature der Antikörper. *Z. Physiol. Chem* **192**, 45–57 (1930).
2. Pauling, L. A theory of the structure and process of formation of antibodies. *J. Am. Chem. Soc.* **62**, 2643–2657 (1940).
3. Jerne, N.K. The natural selection theory of antibody formation. *Proc. Natl. Acad. Sci. USA* **41**, 849–857 (1955).
4. Burnet, F.M. *The Clonal Selection Theory of Acquired Immunity* 53–61 (Vanderbilt Univ. Press, Nashville, Tennessee, USA, 1959).
5. Lederberg, J. Genes and antibodies. *Science* **129**, 1649–1653 (1959).
6. Talmage, D.W. Immunological specificity. *Science* **129**, 1643–1648 (1959).
7. Tonegawa, S. Somatic generation of antibody diversity. *Nature* **302**, 575–581 (1983).
8. Cygler, M., Rose, D.R. & Bundle, D.R. Recognition of a cell-surface oligosaccharide of pathogenic *Salmonella* by an antibody Fab fragment. *Science* **253**, 442–445 (1991).
9. Zdanov, A. *et al.* Structure of a single-chain antibody variable domain (Fv) fragment complexed with a carbohydrate antigen at 1.7-Å resolution. *Proc. Natl. Acad. Sci. USA* **91**, 6423–6427 (1994).
10. Jeffrey, P.D. *et al.* The X-ray structure of an anti-tumour antibody in complex with antigen. *Nat. Struct. Biol.* **2**, 466–471 (1995).
11. Villeneuve, S. *et al.* Crystal structure of an anti-carbohydrate antibody directed against *Vibrio cholerae* O1 in complex with antigen: molecular basis for serotype specificity. *Proc. Natl. Acad. Sci. USA* **97**, 8433–8438 (2000).
12. Vyas, N.K. *et al.* Molecular recognition of oligosaccharide epitopes by a monoclonal Fab specific for *Shigella flexneri* Y lipopolysaccharide: X-ray structures and thermodynamics. *Biochemistry* **41**, 13575–13586 (2002).
13. Nurminen, M., Leinonen, M., Saikku, P. & Makela, P.H. The genus-specific antigen of *Chlamydia*: resemblance to the lipopolysaccharide of enteric bacteria. *Science* **220**, 1279–1281 (1983).
14. Strain, S.M., Fesik, S.W. & Armitage, I.M. Characterization of lipopolysaccharide from a heptoseless mutant of *Escherichia coli* by carbon 13 nuclear magnetic resonance. *J. Biol. Chem.* **258**, 2906–2910 (1983).
15. Brade, H. & Rietschel, E.T. α(2→4)-interlinked 3-deoxy-D-manno-octulosonic acid disaccharide. A common constituent of enterobacterial lipopolysaccharides. *Eur. J. Biochem.* **145**, 231–236 (1984).
16. Brade, L., Rozalski, A., Kosma, P. & Brade, H. A monoclonal antibody recognizing the 3-deoxy-D-manno-oct-2-ulosonic acid (Kdo) trisaccharide αKdo(2→4)αKdo(2→4) αKdo of *Chlamydophila psittaci* 6BC lipopolysaccharide. *J. Endotoxin Res.* **6**, 361–368 (2000).
17. Schachter, J. & Dawson, C.R. The epidemiology of trachoma predicts more blindness in the future. *Scand. J. Infect. Dis. Suppl.* **69**, 55–62 (1990).
18. Morell, V. Attacking the causes of "silent" infertility. *Science* **269**, 775–777 (1995).
19. de la Maza, L.M., Pal, S., Khamesipour, A. & Peterson, E.M. Intravaginal inoculation of mice with the *Chlamydia trachomatis* mouse pneumonitis biovar results in infertility. *Infect. Immun.* **62**, 2094–2097 (1994).
20. Kuo, C.C., Jackson, L.A., Campbell, L.A. & Grayston, J.T. *Chlamydia pneumoniae* (TWAR). *Clin. Microbiol. Rev.* **8**, 451–461 (1995).
21. Hahn, D.L., Bukstein, D., Luskin, A. & Zeitz, H. Evidence for *Chlamydia pneumoniae* infection in steroid-dependent asthma. *Ann. Allergy Asthma Immunol.* **80**, 45–49 (1998).

22. Bachmaier, K. *et al. Chlamydia* infections and heart disease linked through antigenic mimicry. *Science* **283**, 1335–1339 (1999).
23. Grayston, J.T. Background and current knowledge of *Chlamydia pneumoniae* and atherosclerosis. *J. Infect. Dis.* **181** (suppl. 3), S402–S410 (2000).
24. Kalayoglu, M.V. *et al.* Chlamydial virulence determinants in atherogenesis: the role of chlamydial lipopolysaccharide and heat shock protein 60 in macrophage-lipoprotein interactions. *J. Infect. Dis.* **181** (Suppl 3), S483–S489 (2000).
25. Yucesan, C. & Sriram, S. *Chlamydia pneumoniae* infection of the central nervous system. *Curr. Opin. Neurol.* **14**, 355–359 (2001).
26. McCabe, W.R., Bruins, S.C., Craven, D.E. & Johns, M. Cross-reactive antigens: their potential for immunization-induced immunity to Gram-negative bacteria. *J. Infect. Dis.* **136** (suppl.), S161–S166 (1977).
27. Michael, J.G. & Mallah, I. Immune response to parental and rough mutant strains of *Salmonella minnesota*. *Infect. Immun.* **33**, 784–787 (1981).
28. Heumann, D., Baumgartner, J.D., Jacot-Guillarmod, H. & Glauser, M.P. Antibodies to core lipopolysaccharide determinants: absence of cross-reactivity with heterologous lipopolysaccharides. *J. Infect. Dis.* **163**, 762–768 (1991).
29. Fu, Y., Baumann, M., Kosma, P., Brade, L. & Brade, H. A synthetic glycoconjugate representing the genus-specific epitope of chlamydial lipopolysaccharide exhibits the same specificity as its natural counterpart. *Infect. Immun.* **60**, 1314–1321 (1992).
30. Muller-Loennies, S. *et al.* Characterization of high-affinity monoclonal antibodies specific for chlamydial lipopolysaccharide. *Glycobiology* **10**, 121–130 (2000).
31. Nguyen, H.P. *et al.* Crystallization and preliminary X-ray diffraction analysis of two homologous antigen-binding fragments in complex with different carbohydrate antigens. *Acta Crystallogr. D* **57**, 1872–1876 (2001).
32. Janeway, C. *Immunobiology: The Immune System in Health and Disease* xviii, 732 (Garland, New York, 2001).
33. Li, Y., Li, H., Yang, F., Smith-Gill, S.J. & Mariuzza, R.A. X-ray snapshots of the maturation of an antibody response to a protein antigen. *Nat. Struct. Biol.* **10**, 482–488 (2003).
34. Hartman, A.B. & Rudikoff, S. V_H genes encoding the immune response to β-(1,6)-galactan: somatic mutation in IgM molecules. *EMBO J.* **3**, 3023–3030 (1984).
35. Perlmutter, R.M. *et al.* Multiple V_H gene segments encode murine antistreptococcal antibodies. *J. Exp. Med.* **159**, 179–192 (1984).
36. Kearney, J.F., Cooper, M.D. & Lawton, A.R. B cell differentiation induced by lipopolysaccharide. IV. Development of immunoglobulin class restriction in precursors of IgG-synthesizing cells. *J. Immunol.* **117**, 1567–1572 (1976).
37. Barrett, D.J. & Ayoub, E.M. IgG_2 subclass restriction of antibody to pneumococcal polysaccharides. *Clin. Exp. Immunol.* **63**, 127–134 (1986).
38. Silberstein, L.E. *et al.* Variable region gene analysis of pathologic human autoantibodies to the related i and I red blood cell antigens. *Blood* **78**, 2372–2386 (1991).
39. Foote, J. & Milstein, C. Conformational isomerism and the diversity of antibodies. *Proc. Natl. Acad. Sci. USA* **91**, 10370–10374 (1994).
40. Wedemayer, G.J., Patten, P.A., Wang, L.H., Schultz, P.G. & Stevens, R.C. Structural insights into the evolution of an antibody combining site. *Science* **276**, 1665–1669 (1997).
41. Schultz, P.G. & Lerner, R.A. Completing the circle. *Nature* **418**, 485 (2002).
42. Chothia, C. & Lesk, A.M. Canonical structures for the hypervariable regions of immunoglobulins. *J. Mol. Biol.* **196**, 901–917 (1987).
43. Chothia, C. *et al.* Structural repertoire of the human V_H segments. *J. Mol. Biol.* **227**, 799–817 (1992).
44. Barre, S., Greenberg, A.S., Flajnik, M.F. & Chothia, C. Structural conservation of hypervariable regions in immunoglobulins evolution. *Nat. Struct. Biol.* **1**, 915–920 (1994).
45. Tomlinson, I.M., Cox, J.P., Gherardi, E., Lesk, A.M. & Chothia, C. The structural repertoire of the human Vκ domain. *EMBO J.* **14**, 4628–4638 (1995).
46. Al-Lazikani, B., Lesk, A.M. & Chothia, C. Standard conformations for the canonical structures of immunoglobulins. *J. Mol. Biol.* **273**, 927–948 (1997).
47. Morea, V., Tramontano, A., Rustici, M., Chothia, C. & Lesk, A.M. Conformations of the third hypervariable region in the V_H domain of immunoglobulins. *J. Mol. Biol.* **275**, 269–294 (1998).
48. Sharon, J. Structural correlates of high antibody affinity: three engineered amino acid substitutions can increase the affinity of an anti-*p*-azophenylarsonate antibody 200-fold. *Proc. Natl. Acad. Sci. USA* **87**, 4814–4817 (1990).
49. Shirai, H., Kidera, A. & Nakamura, H. Structural classification of CDR-H3 in antibodies. *FEBS Lett.* **399**, 1–8 (1996).
50. Shirai, H., Nakajima, N., Higo, J., Kidera, A. & Nakamura, H. Conformational sampling of CDR-H3 in antibodies by multicanonical molecular dynamics simulation. *J. Mol. Biol.* **278**, 481–496 (1998).
51. Brade, H., Brade, L. & Nano, F.E. Chemical and serological investigations on the genus-specific lipopolysaccharide epitope of *Chlamydia*. *Proc. Natl. Acad. Sci. USA* **84**, 2508–2512 (1987).
52. Holst, O., Bock, K., Brade, L. & Brade, H. The structures of oligosaccharide bisphosphates isolated from the lipopolysaccharide of a recombinant *Escherichia coli* strain expressing the gene *gseA* [3-deoxy-D-manno-octulopyranosonic acid (Kdo) transferase] of *Chlamydia psittaci* 6BC. *Eur. J. Biochem.* **229**, 194–200 (1995).
53. Otwinowski, Z. & Minor, W. Processing of X-ray diffraction data collected in oscillation mode. *Methods Enzymol.* **276**, 307–326 (1996).
54. Brunger, A.T. *et al.* Crystallography & NMR system: a new software suite for macromolecular structure determination. *Acta Crystallogr. D* **54**, 905–921 (1998).
55. Rose, D.R. *et al.* Crystal structure to 2.45 Å resolution of a monoclonal Fab specific for the *Brucella* A cell wall polysaccharide antigen. *Protein Sci.* **2**, 1106–1113 (1993).
56. Evans, S.V., Rose, D.R., To, R., Young, N.M. & Bundle, D.R. Exploring the mimicry of polysaccharide antigens by anti-idiotypic antibodies. The crystallization, molecular replacement, and refinement to 2.8 Å resolution of an idiotope-anti-idiotope Fab complex and of the unliganded anti-idiotope Fab. *J. Mol. Biol.* **241**, 691–705 (1994).
57. Evans, S.V. SETOR: hardware-lighted three-dimensional solid model representations of macromolecules. *J. Mol. Graph.* **11**, 127–128, 134–138 (1993).
58. Martin, A.C. Accessing the Kabat antibody sequence database by computer. *Proteins* **25**, 130–133 (1996).